nature COMMUNICATIONS

ARTICLE

https://doi.org/10.1038/s41467-019-08495-5 OPEN

Highly emissive excitons with reduced exchange energy in thermally activated delayed fluorescent molecules

Anton Pershin[1], David Hall[1,2], Vincent Lemaur[1], Juan-Carlos Sancho-Garcia[3], Luca Muccioli[4], Eli Zysman-Colman[2], David Beljonne[1] & Yoann Olivier[1]

Unlike conventional thermally activated delayed fluorescence chromophores, boron-centered azatriangulene-like molecules combine a small excited-state singlet-triplet energy gap with high oscillator strengths and minor reorganization energies. Here, using highly correlated quantum-chemical calculations, we report this is driven by short-range reorganization of the electron density taking place upon electronic excitation of these multi-resonant structures. Based on this finding, we design a series of π-extended boron- and nitrogen-doped nanographenes as promising candidates for efficient thermally activated delayed fluorescence emitters with concomitantly decreased singlet-triplet energy gaps, improved oscillator strengths and core rigidity compared to previously reported structures, permitting both emission color purity and tunability across the visible spectrum.

[1] Laboratory for Chemistry of Novel Materials, University of Mons, Place du Parc 20, B-7000 Mons, Belgium. [2] Organic Semiconductor Centre, EaStCHEM School of Chemistry, University of St Andrews, St Andrews KY16 9ST, United Kingdom. [3] Departamento de Química Física, Universidad de Alicante, E-03080 Alicante, Spain. [4] Dipartimento di Chimica Industriale "Toso Montanari", Università di Bologna, I-40136 Bologna, Italy. Correspondence and requests for materials should be addressed to Y.O. (email: Yoann.OLIVIER@umons.ac.be)

The discovery of purely organic thermally activated delayed fluorescence (TADF) materials, with its premise to break the spin statistical bottleneck of 25% internal quantum efficiency without the requirement of rare noble metal emitters, has prompted a paradigm shift in the design of emitter materials for use in organic light-emitting diodes (OLEDs)[1]. TADF is rooted in a thermally promoted reverse intersystem crossing (RISC) process enabling upconversion of triplet excitons into emissive singlet excitons, which otherwise would be lost through non-radiative pathways. One key property TADF molecules should fulfill for efficient RISC is a small energy gap between the lowest singlet and triplet excited states ΔE_{ST} (usually < 0.2 eV), so that delayed fluorescence can be thermally activated at room temperature (though exceptions to this general rule exist that involve higher-lying triplet states)[2]. The most widely applied design strategy so far is based on molecules featuring weakly coupled and spatially separated donor (D) and acceptor (A) moieties. This motif sustains charge-transfer (CT) excitations with small exchange interactions and correspondingly small ΔE_{ST} compared to localized excited states[3–5].

However, this approach suffers from a number of drawbacks that directly reflect the nature of the emissive excited state. In particular, achieving high photoluminescence quantum yields (PLQY) and color purity in conventional TADF molecule-based OLEDs has been challenging thus far[6–9]. As a consequence of their dominant CT character, the singlet electronic excitations in these molecules often display fairly small radiative emission cross-sections (oscillator strengths, f_{osc}). Hence, high PLQY in these materials is only possible through efficient suppression of non-radiative decay processes. Moreover, charge-transfer excitations are usually accompanied by large structural reorganization, associated with conformational degrees of freedom in D-A molecular architectures, leading to broad emission spectra. Yet, such conformational gating effects also feed small admixtures of local (covalent) excited-state character into (primarily triplet) CT (ionic) excitations, prompting the needed spin-orbit interaction that mediates spin conversion[10–13]. Thus, designing optimally performing TADF compounds in this scenario relies on the necessarily delicate balance between antagonistic effects.

A notable departure from the usual strategy has recently been proposed by Hatakeyama et al.[6,7,14] who designed TADF emitters as triangulene cores incorporating *ortho*-substituted boron and nitrogen atoms to promote multiple resonance effects (see chemical structures in Fig. 1 and resonant structures in Supplementary Fig. 5). Unlike conventional D-A architectures, these boron-centered azatriangulenes yield concomitantly narrow emission spectra (full-width at half-maximum = 28 nm), relatively large f_{osc} (~0.2 for both **DABNA-1** and **2**) and small ΔE_{ST} (~0.15 eV for **DABNA-1** and 0.21 for **2**) values. OLEDs with high maximum external quantum efficiencies (EQE_{max}) of 13.5% and pure blue emission [CIE coordinates of (0.13, 0.09] for **DABNA-1** were demonstrated. In marked contrast with experiment, recent publications[5,15,16] reported Time-Dependent Density Functional Theory (TD-DFT) ΔE_{ST} predictions in the range 0.4–0.6 eV depending on functional, largely overestimating the experimental values. Based on these TD-DFT calculations, two mechanistic pictures for TADF in boron-centered azatriangulenes molecules have been put forward: Lin et al.[15] claimed that RISC occurs directly from T_1 to S_1 while Northey et al. advanced that RISC involves an intermediate higher-lying triplet state T_2[16].

Here, by scrutinizing the nature of the lowest electronic excitations in these molecules, we propose a new paradigm for TADF that builds on the concept of short-range charge-transfer illustrated in Fig. 1. While long-distance charge separation in multichromophoric D-A systems reduces ΔE_{ST} at the expense of f_{osc}, we show that boron-centered azatriangulenes undergo a large

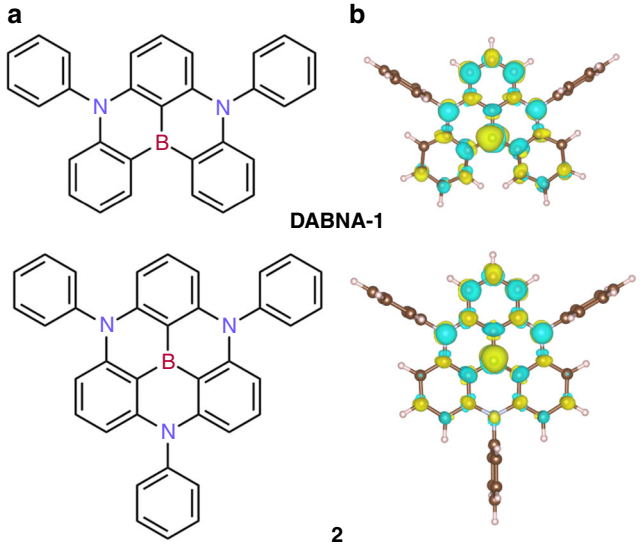

Fig. 1 Evidence for short-range charge transfer in boron-centered azatriangulene molecules. **a** Chemical structures and **b** difference density plots of **DABNA-1** and **2** (summing over the two doubly degenerated S_1 states, see Supplementary Fig. 4). Yellow (blue) color indicates increased (decreased) electron density upon S_0-S_1 excitation

but local spatial reorganization of the electronic density in the excited states, which significantly lowers the exchange energy while maintaining high overlap between wavefunction tails and therefore high f_{osc} transitions, together with small structural relaxation energies. Based on these results, we propose analogs that we hope will lead to high performance TADF emitters in OLED devices.

Results

Origin of small ΔE_{ST} in DABNA molecules. We start our analysis with **DABNA-1**[6]. Irrespective of the choice of the DFT functional and the use (or not) of the Tamm-Dancoff approximation, all our TD-DFT calculations yield erroneously large ΔE_{ST} values (e.g., 0.56 eV at B3LYP level), in line with refs. [6,15,16] (see Supplementary Table 1). The use of tuned range-separated functionals does not help either. By varying the amount of Hartree-Fock-like exchange in the functional, we observe a smooth decrease of ΔE_{ST} that reaches a more reasonable 0.25 eV with pure semilocal models (e.g., LDA), but at the cost of an unphysical delocalization of the electronic density over the outer phenyl rings (Supplementary Fig. 1). The discrepancy between experiment and theory has more fundamental grounds, as we discovered by running higher-level Spin-Component Scaling second-order approximate Coupled-Cluster (SCS-CC2) calculations with the def2-TZVP basis set (see SI for further details on these calculations).

In contrast to TD-DFT, SCS-CC2 calculations on **DABNA-1** and compound **2** provide (vertical, i.e., based on ground-state geometry) ΔE_{ST} values in excellent agreement with experiments, Table 1. Despite relatively small ΔE_{ST} values (<0.2 eV), the lowest singlet electronic excitation in these molecules is strongly dipole-allowed with a f_{osc} of 0.31 in **DABNA-1** and (summing over the two degenerated singlet excited states arising from the C_{3V}-symmetry) 0.26 in **2**. Most interestingly, similar ΔE_{ST} values were obtained for vertical and adiabatic (fully relaxed) excitations, owing to modest nuclear reorganization energies in the S_1 state (0.12 eV and 0.10 eV for **DABNA-1** and molecule **2**, respectively, Table 1), which should ensure narrow singlet emission as an added virtue.

Table 1 Excited state properties

Molecule	*n*	S_0->S_n	S_0->T_n	ΔE_{ST} (vert)	ΔE_{ST} (adiab)	ΔE_{ST} (exp)	f_{osc}	λ_{reorg}
DABNA-1	1	3.25	3.10	0.15	0.15	0.15[6]	0.31	0.12
	2	4.23	3.75					
	3	4.28	3.87					
2	1*	3.67	3.50	0.17	0.20	0.21[7]	0.13	0.10
	2	4.15	3.74					

Vertical excitation energies for the three lowest-lying triplet and singlet excited states, singlet-triplet energy differences (ΔE_{ST}) for the vertical and adiabatic transitions, oscillator strengths (f_{osc}), and S_0->S_1 reorganization energies (λ_{reorg}) obtained for **DABNA-1** and compound **2** with the SCS-CC2 method
*S_1 and T_1 are doubly degenerate. All energies are given in eV

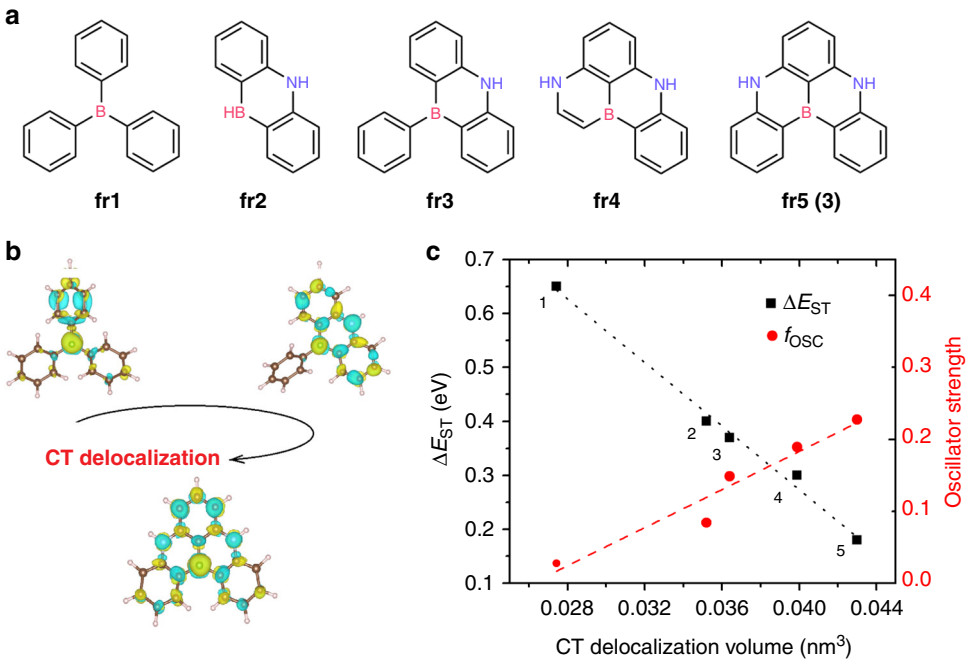

Fig. 2 Charge transfer delocalization helps in decreasing the singlet-triplet energy gap and increasing the oscillator strength. **a** Chemical structures of DABNA-1 fragments. **b** Difference density plots computed for selected fragments from **a**. **c** ΔE_{ST} (black squares) and oscillator strengths, f_{osc} (red dots) as a function of CT delocalization volume for the selected set of fragments

The origin for the unusual electronic properties of these molecules is best pictured by difference density plots for the S_0-S_1 and S_0-T_1 excitations, calculated at the SCS-CC2 level and shown in Fig. 1b for **DABNA-1** (cf. Supplementary Fig. 1). These plots reveal a remarkably homogenous short-distance reshuffling of the electronic density upon excitation that yields spatially alternating hole-rich and electron-rich regions. The density reorganization is partly shaped by second-order electronic correlation effects (Supplementary Fig. 2) and thus, not surprisingly, cannot be fully captured at the (one-electron) TD-DFT level. To elucidate further the origin for the small ΔE_{ST} in **DABNA-1** and **2**, it is instructive to analyze the results obtained for fragments (labeled **fr1**–**fr5** in Fig. 2a) extracted from the parent molecules. Close inspection of the differential density plots for both singlet and triplet excitations show the same alternating pattern as the one observed for **DABNA-1**, yet with an increasing spreading in space as the fragment becomes larger and/or more conjugated, Fig. 2b. This effect can be quantitatively assessed by computing the CT delocalization volume (see Supplementary Information "Difference density plots" section for computational details). Figure 2c shows strong linear correlations ($R^2 = 0.99$) between both ΔE_{ST} or f_{osc} and the CT volume, with more extended systems providing, remarkably, smaller ΔE_{ST} and larger f_{osc}. The trend is in fact reminiscent of the behavior of localized (covalent) excitations in conjugated materials, where the exchange energy measured/calculated in polymer chains is usually significantly smaller than that in the parent small molecules[17].

Highly emissive molecules with small ΔE_{ST}. The most striking feature arising from Fig. 2c is that while CT delocalization triggers a large decrease in ΔE_{ST} from **fr1** (0.65 eV) to **fr5** (0.18 eV), the lowest excitation f_{osc} strength instead increases along the same sequence, from 0.02 in **fr1** to 0.23 in **fr5**. This result contrasts with the behavior observed for conventional D-A-based TADF molecular architectures[12]. Inspired by this finding, we applied the multiple charge resonance strategy to design in silico new TADF chromophores based on π-extended B-doped and N-doped nanographenes (Fig. 3a). The results reported in Fig. 3b confirm the trends observed for the fragments in Fig. 2, i.e., reduced ΔE_{ST} (as supported by the Zero Field Splitting calculations, see Supplementary Table 4) and enhanced f_{osc}. In the largest compound investigated, **6**, the singlet and triplet excitations are found to be quasi-degenerate (ΔE_{ST} ~3 meV), yet the singlet f_{osc} is as large as 1.0. Moreover, as all investigated molecules have a rigid backbone with small (intramolecular) nuclear reorganization

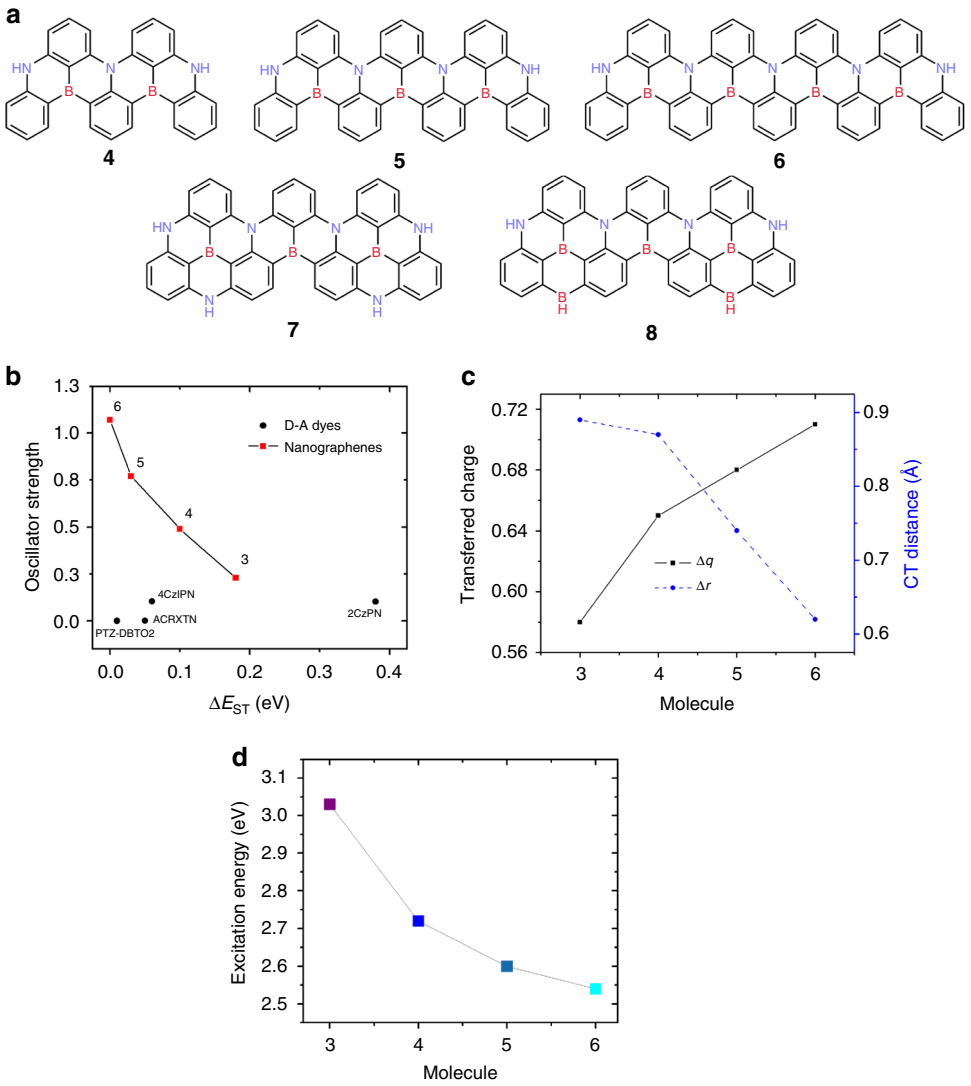

Fig. 3 Excited state properties for the designed boron-doped and nitrogen-doped π-extended nanographenes. **a** Chemical structures of engineered molecules **4–8**. Compound **3** coincides with **fr5** in Fig. 2a. **b** Oscillator strength, f_{osc}, as a function of ΔE_{ST} for **3–6** (red squares) against conventional D-A reference TADF emitters (black dots, see chemical structures in Supplementary Fig. 3). **c** Transferred charge (in |e|) and CT distance (Å), as computed for molecules **3–6**. **d** Emission energies and respective colors for **3–6**

energies (Supplementary Table 3), we expect these give rise to narrow linewidth and pure color emission. It is important to stress that the increment in f_{osc} is not solely caused by the increase of the number of π-electrons but, instead, occurs primarily through extended delocalization of the wavefunction and increased polarizability along the main-axis of the molecules.

Additional insights into this unexpected behavior can be gained from a detailed analysis of the singlet excited-state wavefunctions, in particular of the following two metrics that assess the relative electron-hole quasi-particles: the electron-hole separation (Δr) and the amount of charge transferred (Δq). Figure 3c points to a picture where the low-lying singlet excited state undergoes substantial reshuffling of the electronic density (large Δq values) but over short distances (small Δr values). Besides, these characteristics get more pronounced as the ribbons grow longer: Δr decreases from 0.9 to 0.6 Å when going from **3** to **6**, while Δq increases from 0.58 |e| in **3** up to 0.71 |e| in **6**. The resulting 'short-range/local CT' states feature both high electron-hole wavefunction overlaps and small exchange interactions, turning into high f_{osc} and low ΔE_{ST} values for the DABNA core building block. In addition, 'long-range' π-conjugation along ribbons **3–6** translates into electronic excitations with extended delocalization and hence increased polarizability and radiative decay rates. While none of these effects is surprising when taken separately, it is the combination of short-range charge separation and long-range electronic delocalization that makes these molecules unique. We believe this is a real breakthrough as most of the low ΔE_{ST} TADF molecules reported so far are characterized by very low f_{osc} and radiative decay rates. This is exemplified by the comparison of compounds **3–6** with selected D-A TADF reference molecules, for which f_{osc} and ΔE_{ST} calculated at a similar level of theory (Fig. 3b and Supplementary Table 2) are concurrently small, in line with their Δr values larger than the 1.5–2.0 Å criterion usually set to discriminate CT excitations[18] that we reported previously[12].

Finally, besides the beneficial effect on ΔE_{ST} and f_{osc}, increased delocalization along the series **3–6** expectedly produces a spectral red-shift of the lowest singlet excitation, thereby allowing for variations of the emission color from blue to green as a function of the molecular size (Fig. 3d). Further tuning of the emission

wavelength can be achieved, for instance by introducing an excess amount of N-atoms or B-atoms into the conjugated plane. For the sake of illustration, we designed two other molecules, **7** and **8**, based on **5**. These chromophores essentially retain the properties of the parent molecule in terms of ΔE_{ST} and f_{osc} (see Supplementary Table 3), however, they possess emission wavelengths blue-shifted to 2.85 eV (435 nm, deep blue, **7**) and red-shifted to 2.1 eV (590 nm, yellow, **8**) compared to **5**.

To conclude, using highly correlated wavefunction-based methods, we have elucidated the origin for the reduced singlet-triplet gap in the boron-centered azatriangulene molecules originally reported by Hatakeyama et al. as resulting from a local alternating rearrangement of the electronic density upon excitation. We have further shown that this is compatible with high absorption and emission extinction coefficients and we have proposed a strategy, based on promoting short-range charge-transfer in π-extended chromophores, as a way to simultaneously optimize RISC and radiative decay rates. This approach has been successfully applied to the design of TADF molecules with: (i) close-to-resonant lowest singlet and triplet excited states; (ii) large singlet radiative decay rates; (iii) tunable and expected pure color singlet emission. We hope our theoretical work will catalyze the synthesis and trigger the characterization of a new generation of TADF molecules with unprecedented electroluminescence quantum efficiencies.

Methods

Computational details. The SCS-CC2 calculations were performed by the TURBOMOLE 6.5 software[19] using the spin-adapted formulation of the linear response theory and the def2-TZVP basis set[20]. The TD-DFT calculations were carried out using the def2-TZVP basis set. The TD-DFT calculations together with the respective analysis, were performed with the ORCA 4.0.1.2 software[21].

Data availability

All data are available from the corresponding author upon request.

Received: 4 July 2018 Accepted: 4 January 2019
Published online: 05 February 2019

References

1. Endo, A. et al. Efficient up-conversion of triplet excitons into a singlet state and its application for organic light emitting diodes. *Appl. Phys. Lett.* **98**, 2011–2014 (2011).
2. Gan, L. et al. Achieving efficient triplet exciton utilization with large ΔE_{ST} and nonobvious delayed fluorescence by adjusting excited state energy levels. *J. Phys. Chem. Lett.* **9**, 4725–4731 (2018).
3. Uoyama, H., Goushi, K., Shizu, K., Nomura, H. & Adachi, C. Highly efficient organic light-emitting diodes from delayed fluorescence. *Nature* **492**, 234–238 (2012).
4. Wong, M. Y. & Zysman-Colman, E. Purely organic thermally activated delayed fluorescence materials for organic light-emitting diodes. *Adv. Mater.* **29**, 1605444 (2017).
5. Liu, Y., Li, C., Ren, Z., Yan, S. & Bryce, M. R. All-organic thermally activated delayed fluorescence materials for organic light-emitting diodes. *Nat. Rev. Mater.* **3**, 18020 (2018).
6. Hatakeyama, T. et al. Ultrapure blue thermally activated delayed fluorescence molecules: efficient HOMO-LUMO separation by the multiple resonance effect. *Adv. Mater.* **28**, 2777–2781 (2016).
7. Nakatsuka, S., Gotoh, H., Kinoshita, K., Yasuda, N. & Hatakeyama, T. Divergent synthesis of heteroatom-centered 4,8,12-triazatriangulenes. *Angew. Chem. Int. Ed.* **56**, 5087–5090 (2017).
8. Godumala, M., Choi, S., Cho, M. J. & Choi, D. H. Thermally activated delayed fluorescence blue dopants and hosts: from the design strategy to organic light-emitting diode applications. *J. Mater. Chem. C.* **4**, 11355–11381 (2016).
9. Yang, Z. et al. Recent advances in organic thermally activated delayed fluorescence materials. *Chem. Soc. Rev.* **46**, 915–1016 (2017).
10. Etherington, M. K., Gibson, J., Higginbotham, H. F., Penfold, T. J. & Monkman, A. P. Revealing the spin–vibronic coupling mechanism of thermally activated delayed fluorescence. *Nat. Commun.* **7**, 13680 (2016).
11. Gibson, J., Monkman, A. P. & Penfold, T. J. The importance of vibronic coupling for efficient reverse intersystem crossing in thermally activated delayed fluorescence molecules. *ChemPhysChem* **17**, 2956–2961 (2016).
12. Olivier, Y., Moral, M., Muccioli, L. & Sancho-García, J.-C. Dynamic nature of excited states of donor–acceptor TADF materials for OLEDs: how theory can reveal structure–property relationships. *J. Mater. Chem. C.* **5**, 5718–5729 (2017).
13. Olivier, Y. et al. Nature of the singlet and triplet excitations mediating thermally activated delayed fluorescence. *Phys. Rev. Mater.* **1**, 75602 (2017).
14. Matsui, K. et al. One-shot multiple borylation toward BN-doped nanographenes. *J. Am. Chem. Soc.* **140**, 1195–1198 (2018).
15. Lin, L., Fan, J., Cai, L. & Wang, C. K. Excited state dynamics of new-type thermally activated delayed fluorescence emitters: theoretical view of light-emitting mechanism. *Mol. Phys.* **116**, 19–28 (2018).
16. Northey, T. & Penfold, T. J. The intersystem crossing mechanism of an ultrapure blue organoboron emitter. *Org. Electron. Phys. Mater. Appl.* **59**, 45–48 (2018).
17. Köhler, A. & Beljonne, D. The singlet–triplet exchange energy in conjugated polymers. *Adv. Funct. Mater.* **14**, 11–18 (2004).
18. Guido, C. A. et al. On the metric of charge transfer molecular excitations: a simple chemical descriptor. *J. Chem. Theory Comput.* **9**, 3118–3126 (2013).
19. TURBOMOLE V6.5. A development of University of Karlsruhe and Forschungszentrum Karlsruhe GmbH, 1989-2007, TURBOMOLE GmbH, since 2007. https://www.turbomole.com (2013).
20. Weigend, F. & Ahlrichs, R. Balanced basis sets of split valence, triple zeta valence and quadruple zeta valence quality for H to Rn: Design and assessment of accuracy. *Phys. Chem. Chem. Phys.* **7**, 3297 (2005).
21. Neese, F. Software update: the ORCA program system, version 4.0. *Wiley Interdiscip. Rev. Comput. Mol. Sci.* **8**, e1327 (2018).

Acknowledgements

The work was supported by the European Union's Horizon 2020 research and innovation program under Grant Agreement N°. 646176 (EXTMOS project). A.P. acknowledges the financial support from the Marie Curie Fellowship (MILORD project, N°. 748042). Computational resources have been provided by the Consortium des Équipements de Calcul Intensif (CÉCI), funded by the Fonds de la Recherche Scientifiques de Belgique (F.R.S.-FNRS) under Grant No. 2.5020.11, as well as the Tier-1 supercomputer of the Fédération Wallonie-Bruxelles, infrastructure funded by the Walloon Region under the grant agreement n1117545. The St Andrews team would like to thank the Leverhulme Trust (RPG-2016-047) and EPSRC (EP/P010482/1) for financial support.

Author contributions

The calculations were performed by A.P. with contributions from D.H. and Y.O. The manuscript was written by A.P., D.H., V.L., J.-C.S.-G., L.M., E.Z.-C., D.B., and Y.O. contributed to the analysis and improvements of the work.

Additional information

Supplementary Information accompanies this paper at https://doi.org/10.1038/s41467-019-08495-5.

Competing interests: The authors declare no competing interests.

Reprints and permission information is available online at http://npg.nature.com/reprintsandpermissions/

Journal peer review information: *Nature Communications* thanks the anonymous reviewers for their contribution to the peer review of this work.

Publisher's note: Springer Nature remains neutral with regard to jurisdictional claims in published maps and institutional affiliations.